Synthesis, Spectroscopic Characterization and Photophysics of a Novel Environmentally Sensitive Dye 3-Naphthyl-1-phenyl-5-(4-carboxyphenyl)-2-pyrazoline

ARTICLE *in* JOURNAL OF LUMINESCENCE · FEBRUARY 2015

Impact Factor: 2.72 · DOI: 10.1016/j.jlumin.2014.10.045

4 AUTHORS:

Beena Varghese
Sultan Qaboos University
4 PUBLICATIONS **4** CITATIONS
SEE PROFILE

Saleh Al Busafi
Sultan Qaboos University
22 PUBLICATIONS **113** CITATIONS
SEE PROFILE

FakhrEldin O. Suliman
Sultan Qaboos University
99 PUBLICATIONS **840** CITATIONS
SEE PROFILE

Salma Mohamed Al-Kindy
Sultan Qaboos University
77 PUBLICATIONS **524** CITATIONS
SEE PROFILE

Journal of Luminescence 159 (2015) 9–16

Contents lists available at ScienceDirect

Journal of Luminescence

journal homepage: www.elsevier.com/locate/jlumin

Synthesis, spectroscopic characterization and photophysics of a novel environmentally sensitive dye 3-naphthyl-1-phenyl-5-(4-carboxyphenyl)-2-pyrazoline

Beena Varghese, Saleh N. Al-Busafi, FakhrEldin O. Suliman *, Salma M.Z. Al-Kindy *

Department of Chemistry, College of Science, Sultan Qaboos University, Box 36, Al-khod 123, Sultanate of Oman

ARTICLE INFO

Article history:
Received 19 July 2014
Received in revised form
9 October 2014
Accepted 20 October 2014
Available online 29 October 2014

Keywords:
Synthesis
Pyrazoline
Charge-transfer character
Fluorescence
Solvent effect
TD-DFT

ABSTRACT

Synthesis and photophysical properties of a novel pyrazoline – containing fluorophore, 3-naphthyl-1-phenyl-5-(4-carboxyphenyl)-2-pyrazoline (NPCP) **A**, and its proline derivative (NPCP-P) **B** are presented in this work. The highlight of this fluorescent dye is that, it can be prepared from available starting material *via* two synthetic steps, easily converted to the corresponding amide derivative by *in situ* nucleophilic acyl substitution of the corresponding acid chloride, and its purification by simple chromatographic techniques. The structures of the new compounds were verified using various spectroscopic tools. Furthermore, photophysical properties of the new fluorophores were studied and interesting solvatochromic behaviour was observed. Due to the presence of proton acceptor linked to the fluorophore, NPCP displays pH-sensitive absorption and fluorescence emission. The interaction of NPCP and NPCP-P with various micelles has been studied by steady state fluorescence. All results reflect the importance of the medium effect on the analytical application of NPCP as a potential fluorescent label for derivatization of analytes having amine ($-NH_2$) group. Theoretical calculations were performed for both compounds using time dependent density functional theory (TD-DFT) at B3LYP/6-31G(d, p) level. The calculations indicate that the exited state dipole moments are larger than those of the ground state in line with the experimental findings.

1. Introduction

The design and development of chemical probes for biological labeling and imaging have been the subject of fascination to scientists which led to the introduction of a profound number of novel molecules that exhibited interesting interaction properties with various biological, chemical and medical systems. Reagents are required with sufficient flexibility in their synthetic strategies, increased quantum yields for fluorescence, longer emission wavelengths, larger stokes shifts and with good photostability.

Pyrazoline is a five-membered heterocyclic compound having two adjacent nitrogen atoms within the ring. In addition to its role as a key precursor for the synthesis of novel organic compounds with medicinal properties, pyrazoline ring compounds show stronger fluorescence because of the double bond hindering which occurred due to cyclization [1–4]. Among various possible fluorescent probes, pyrazoline-based fluorophores stand out due to their simple structure and favorable photophysical properties such as large extinction coefficient and quantum yields. Their attractive properties, including cation or pH-sensitive probes, are known, and the solubility of pyrazoline fluorophores as probes is also explored. Changes in their structure have offered a high degree of diversity that has proven useful for the development of novel probes [1,3,5–8].

On the other hand, interest in naphthalene based fluorophores has grown over the past few years because of their advantageous photophysical properties. Fused heterocyclic systems incorporating the naphthalene moiety and pyrazole ring has been previously synthesized for the purpose of obtaining compounds of biological importance [9]. The synthesis of a new derivative of pyrazoline, 1-phenyl-3-biphenyl-5-(N-ethylcarbazole-3-yl)-2-pyrazoline (PBEP) that show promising applications in the study of DNA has also been reported [7]. Moreover, pyrazoline compounds with biological and medicinal applications have been recently receiving much interest [9–17]. Fluorescence spectra of a series of 1, 3, 5-triaryl-2-pyrazolines indicated that substituents in the 3-phenyl ring resulted in the shifting of fluorescence emission wavelength [18]. Zhenglin and Shinkang have reported that an intramolecular conjugated charge transfer process exists in pyrazoline moiety in the excited state [19]. N-phenyl substituted 2-pyrazoline and its derivative show interesting photophysical properties due to the

* Corresponding authors. Tel.: +968 24141480; fax: +968 24141469.
E-mail addresses: fsuliman@squ.edu.om (F.O. Suliman), alkindy@squ.edu.om (S.M.Z. Al-Kindy).

http://dx.doi.org/10.1016/j.jlumin.2014.10.045
0022-2313/

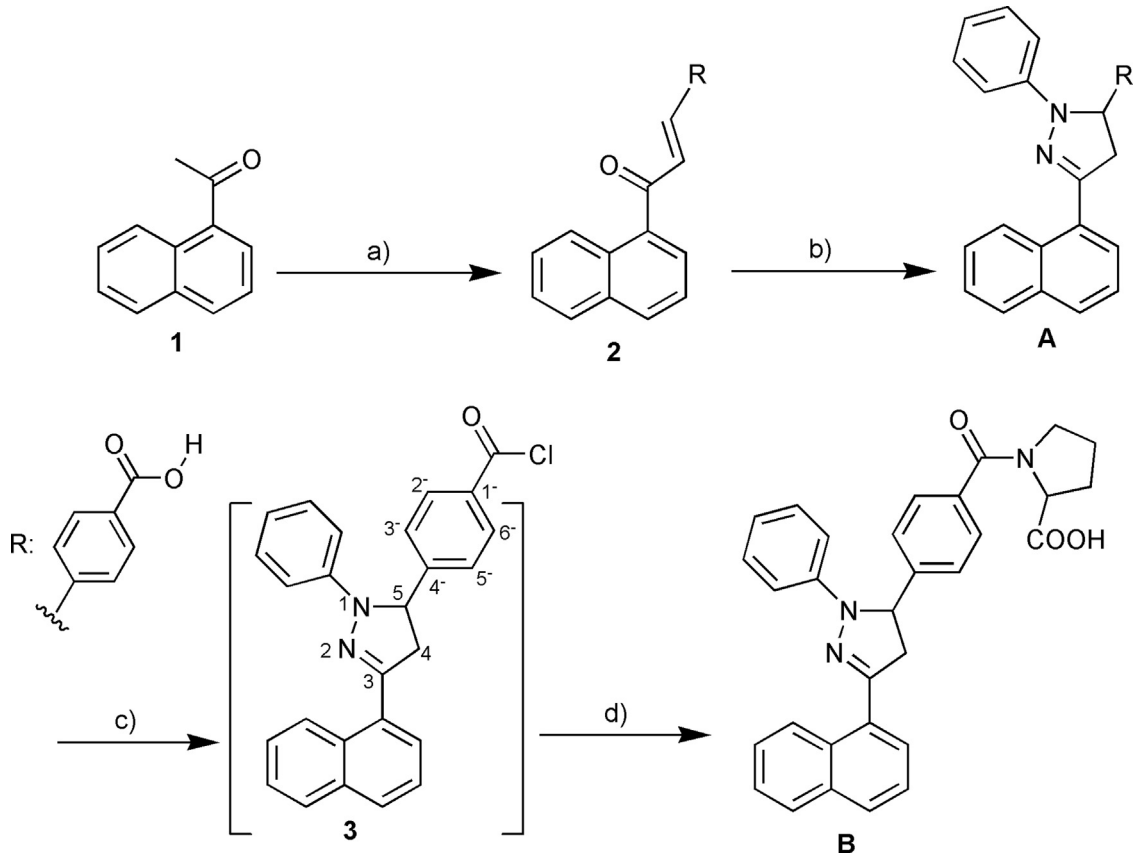

Scheme 1. Reaction conditions (a) 4-formyl benzoic acid, KOH, EtOH, reflux, and 2 h, (b) phenyl hydrazine, EtOH, reflux, 3 h, and dilute sulfuric acid, (c) thionyl chloride, benzene, reflux, 1 h (d) proline, acetonitrile, borate buffer, and reflux.

presence of electron donors and acceptors at N (1) and C (3) positions, respectively [20]. Barberá et al. performed a study on the structure-property relationships in a series of 3- (4-n-decyloxyphenyl)-1-(p-X-phenyl)-2-pyrazoline and they found that if the phenyl ring is substituted or non-substituted, the pyrazoline compounds are fluorescent [8].

In this paper, in view of the photophysical properties of pyrazoline – based dyes and our interest in synthesizing analogous compounds involving fascinating diverse heterocycles, we designed and synthesized a novel pyrazoline-based fluorophore (NPCP) containing phenyl substituted pyrazoline ring (electron-donor) as a channel in between naphthalene moiety (electron-acceptor) and electron withdrawing carboxylic group as side chains and its proline derivative (NPCP-P) (Scheme 1). In combination of pyrazoline moiety with the naphthalene ring, we anticipate the formation of a novel probe for the selective and sensitive trace analysis of analytes having amine ($-NH_2$) groups using various separation techniques.

2. Experimental

2.1. General

All the reagents and solvents used in this study were obtained from Sigma-Aldrich Chemical Company and used without further purification.

Melting points were determined using Gallen-Kamp melting point apparatus. The purity of the synthesized compounds was checked by TLC and analyses were carried out on 0.25 mm thick pre coated silica plates (Merk Fertigplatten kieselgel $60F_{254}$). Column chromatography was performed using Merk silica gel 60 (40–63 μm). IR spectra were determined on a Perkin-Elmer FTIR-881 spectrometer (Perkin-Elmer, USA) using KBr pellets. Proton Magnetic Resonance (^{1}H NMR) spectra were recorded using a 400 MHz Bruker spectrometer (Bruker Corp.,UK) and in particular, the proton chemical shifts were assigned on the basis of (^{1}H–^{1}H) COSY (Correlated SpectroscopY). Carbon Magnetic Resonance (^{13}CNMR) spectra were recorded at a 100.4 MHz Bruker spectrometer (Bruker Corp.,UK) and the multiplicities of ^{13}C NMR resonances were determined by DEPT (90,135) experiments. Chemical shifts (δ_c) are quoted in parts per million (ppm) to the nearest 0.1 and 0.01 and are referenced to the solvent peak ($CDCl_3$). High resolution mass spectra were obtained using Waters LCT Premier XE Mass Spectrometer instrument (determined at the University of Sheffield, UK).

A Shimadzu (model multispec-1501) UV–vis spectrophotometer (Shimadzu, Japan) and a Perkin-Elmer (model LS 55) Luminescence spectrometer (Perkin-Elmer, USA) were used to collect absorption and fluorescence spectra, respectively. All measurements were performed repeatedly, and reproducible results were obtained. Relative fluorescence quantum yield (ϕ_f) were determined using quinine sulfate as the reference standard (ϕ_f=0.55 in 0.1 M H_2SO_4) [19]. Lifetime measurements were performed using a Time-Master Fluorescence lifetime spectrometer obtained from Photon Technology International. Excitation was at 380 nm using light emitting diodes. For NPCP and its derivative fluorescence, a cut-off filter (400 nm, Photon Technology International) was used. The system response time as measured from the scattered light was estimated to be approximately 1.5 ns. The observed decays were fitted to multi-exponential functions convoluted with the instrument response function (IRF). The fit was judged by the value of the reduced chi-squared (χ^2) values which were close to unity (0.98–1.2).

2.1.1. Synthesis of 3-naphthyl-1-phenyl-5-(4-carboxyphenyl)-2-pyrazoline (NPCP)

A mixture of 4-((E)-3-(naphthalene-4-yl)-3-oxoprop-1-enyl) benzoic acid (2) (5.0 g, 18.2 mmol) in 100 ml ethanol was added to phenyl hydrazine (4.0 g, 36.5 mmol) and the reaction was heated under reflux for 3 h. After cooling at room temperature, the resulting solution was made acidic by adding dil.H_2SO_4 drop wise followed by the addition of water. The resulting solution was concentrated and the solid was purified by column chromatography using chloroform alone to yield NPCP (3.5 g, 54%) as orange solid. Mp:129.0–130 °C; IR (KBr): υ 1540, 1129, 3029, 1687, 3490 cm^{-1}; ^1H NMR (400 MHz, $CDCl_3$): δ(ppm) 3.38 (dd, J=4.4, 7.2 Hz, 1H,), 4.11 (dd, J =4.4, 12.0 Hz, 1H), 5.36 (dd, J=7.2, 12.0 Hz 1H), 6.84 (m, 1H), 6.95 (m, 1H), 7.11(m, 3H), 7.47 (m, 3H), 7.57(m, 1H), 7.67(m, 2H), 7.86 (m, 3H), 8.08(m, 2 H), 9.53 (d, J =4.0 Hz, 1H);^{13}C NMR (400 MHz, CDCl3): δ(ppm) 45.9 (CH_2), 63.1 (CH), 113.1(CH), 113.5 (CH), 119.6 (CH), 120.7 (CH), 124.8 (CH), 125.2 (CH), 126.2 (2 × CH), 126.3 (CH), 127.4 (CH), 128.6 (CH), 128.7 (CH), 129.1 (2 × CH), 130.5 (CH), 131.2 (CH), 132.8 (–C), 142.5 (–C), 143.7 (–C), 144.5(–C), 144.8 (–C), 147.3 (–C), 148.6 (–C), 171.3 (C═O). HRMS ES+ m/z: $[M+H]^+$ Calcd. 393.1603; found 393.1592.

2.1.2. Synthesis of NPCP-proline derivative

A solution of 3-naphthyl-1-phenyl-5-(4-carboxyphenyl)-2-pyrazoline (NPCP) (1.5 g, 1.27 mmol) in benzene was heated under reflux for one hour with thionyl chloride (1.36 g, 3.81 mmol). After cooling at room temperature, the excess thionyl chloride was removed under vacuum. The resulting acid chloride was dissolved in acetonitrile and proline in 0.01 M borate buffer was added drop by drop to this solution. The reaction mixture was left refluxing for 24 h. After cooling the excess solvent was removed under reduced pressure to yield brown solid. The solid was further purified by column chromatography using chloroform as the eluent to give compound NPCP-P (1.32 g, 63.0%) as yellow solid. MP: 164–166 °C; IR(KBr): υ 1178, 1495, 775, 3715, 1639, 3423 cm^{-1}; ^1H NMR (400 MHz,$CDCl_3$): δ(ppm) 1.68 (m, 1H), 1.95 (m, 1H), 2.16 (m, 1H), 2.29 (m, 1H), 3.31 (m, 2H), 3.53 (m, 1H), 4.03 (m, 1H), 4.16 (m, 1H), 5.28 (m, 1H), 6.86-8.18 (m,15H), 8.63 (d, J =4.0 Hz, 1H), 9.46 (d, J =4.4 Hz, 1H); ^{13}C NMR (400 MHz, CDCl3): δ(ppm) 45.9 (CH_2), 27.7 (CH_2), 45.2 (CH_2), 46.0 (CH_2), 60.6 (CH), 62.8 (CH), 114.3 (CH), 123.4 (CH), 124.5 (CH), 124.8 (CH), 125.4 (CH), 126.0 (2 × CH), 126.3 (CH), 127.2 (CH), 127.6 (CH), 127.6 (CH), 128.2 (CH), 128.6 (2 × CH), 130.4 (CH), 131.6 (CH), 137.2 (–C), 139.6 (–C), 142.3 (–C), 144.8 (–C), 147.8 (–C), 148.4 (–C), 152.1(–C), 170.6 (C═O), 170.8 (C═O). ESI-MS ($M–H$)$^-$ calcd. for $C_{31}H_{27}N_3O_3$: 488.21; found: 488.12.

2.2. Computational details

The ground state geometries molecular structures (S_0) of NPCP and NPCP-P were optimized by the density functional theory (DFT) method using the B3LYP (Becke-three parameter hybrid exchange functional [21] combined with the Lee–Yang–Parr correlation function [22]) employing the 6-31G(d, p) basis set. The first excited state geometry (S_1) molecular structure was optimized by the single configuration interaction (CIS) [23], using the same basis set. Estimates of the electronic transition energies, which include some account of the electron correlation, were obtained using the time-dependent density functional theory (TD-DFT) together with the hybrid B3LYP level of theory and using the 6-31G(d, p) basis set. Absorption spectra were obtained by using the ground state optimized geometry whereas emission energies were obtained considering the CIS optimized structures of the excited state. All the above calculations were performed using *Firefly* 8.0 package [24] which is based on the *Gamess-US* source code [25]. The program *GaussSum* [26] was used to determine the contribution of the exited state configurations to the electronic transitions and to create the spectra by convolution of molecular orbitals. *Gabedit* program (version 2.4.7) [27] was also used to generate the molecular orbital plots and to visualize the computed spectra.

3. Results and discussion

3.1. Synthesis and characterization of compounds NPCP and NPCP-P

The synthetic route of the investigated compounds, named 3-naphthyl-1-phenyl-5-(4-carboxyphenyl)-2-pyrazoline (NPCP), and its proline derivative (NPCP-P) commenced from 1-acetylnaphthalene (**1**) as shown in Scheme 1.

The key intermediate α, β- unsaturated ketone **2** was prepared by adopting the well-known aldol condensation reaction between 1-acetylnaphthalene **(1)** and 4-formylbenzoic acid in the presence of potassium hydroxide. The next step involves Michael addition of phenylhydrazine to compound **2** followed by intramolecular cyclization reaction to yield the fluorogenic reagent NPCP. The key step in this synthetic scheme involves the formation of acid chloride from probe NPCP, which was converted *in-situ* into proline derivative NPCP-P by the addition of amino acid proline. The novel compounds are characterized by IR, NMR and MS spectrometry.

3.2. Absorption and fluorescence spectra

The absorption and fluorescence emission spectra of NPCP and NPCP-P were measured in solvents of different polarity at room temperature. The absorption spectra of NPCP in different solvents are shown in Fig. 1. Moreover, the corresponding spectral data are summarized in Tables 1 and 2. The data reveals the presence of two prominent absorption bands in the UV region depending on the environment of the media and the effect of substituents on the aromatic conjugated π – system. In all solvents the maximum absorption is obtained for the higher energy band. It is well known that pyrazoline compounds are typical intra-molecular charge transfer compounds [28]. Both NPCP and its derivative are large conjugated system because there is a naphthalene moiety in C-3 position of pyrazoline, phenyl group at N-1 position and extension of π – system by incorporating phenyl group to C-5 position with –COOH and unbound electron pair of the nitrogen atom in NPCP-P. The band at the shortest wavelength appearing in the range 270–300 nm is ascribed to π–π* transition of the naphthalene systems of the compounds. This assignment is quite reasonable since λ_{max} of this band is slightly altered on transfer from the probe to

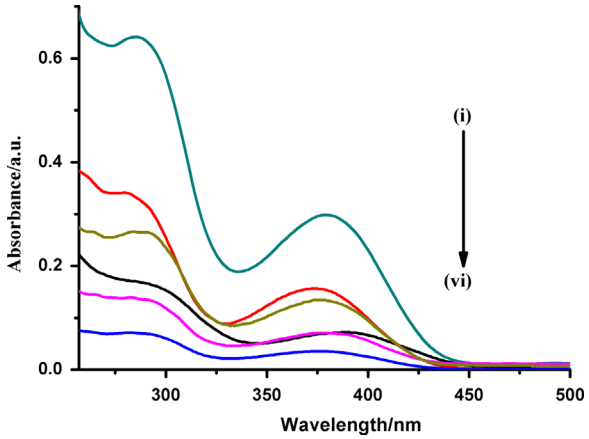

Fig. 1. UV–visible spectra of NPCP-P in different solvents: (i) dioxane, (ii) methanol, (iii) heptane, (iv) water, (v) cyclohexane, and (vi) acetonitrile.

Table 1
Absorption wavelengths and molar absorptivities of NPCP (A) and NPAC-P in various solvents.

Solvent	λ_{abs}(nm)I		λ_{abs}(nm) II		ε (M^{-1} cm^{-1})($\times 10^4$)	
	A	B	A	B	A	B
Water	293	283	383	377	1.3	1.1
Methanol	290	280	379	378	2.5	4.9
Acetonitrile	284	286	372	381	0.93	0.4
Tetrahydrofuran	291	282	366	382	4.4	4.3
1,4-dioxane	290	283	377	384	5.7	6.6
Heptane	277	276	375	365	1.0	1.4
Cyclohexane	273	279	376	363	1.7	1.3

Table 2
Emission wavelength maxima (λ_{max}) quantum yield (Φ_f) lifetime (τ_f) and E_T (30) values for NPCP (A) and NPCP-P (B) in different solvents.

Solvent	λ_{emsn}(nm)		Φ_f		τ_f (ns)		E_T (30)(kcal mol^{-1})
	A	B	A	B	A	B	
Water	491	468	0.17	0.05	1.1	1.05	63.1
Methanol	476	492	0.19	0.12	1.9	0.91	55.4
Acetonitrile	482	506	0.29	0.17	1.6	0.97	46.0
Tetrahydrofuran	469	490	0.48	0.44	1.01	1.06	37.4
1,4-dioxane	465	485	0.55	0.55	0.87	0.81	36.0
Heptane	451	469	0.41	0.23	0.95	1.1	31.1
Cyclohexane	452	482	0.47	0.28	0.86	0.82	30.9

derivative indicating the local nature of such transition. The maximum absorptions ranging from 370 to 400 nm are attributed to π–π^* transition of the conjugated backbone with a considerable charge-transfer character originating mainly from the pyrazoline ring of each compound and pointing towards the naphthalene ring of each compound, thereby enhancing the delocalization of π-electrons throughout the system. The high extinction coefficient values of both compounds suggest that the electronic transition from the ground state to the excited state has a π–π^* character [29].

The emission spectra of both compounds consist of one broad band. This band can be assigned to the $S_1 \rightarrow S_0$ electronic transition. The effect of the polarity of the medium on the fluorescence is more pronounced than that on the absorption spectrum of both compounds. This is because the ICT effect leads to a large dipole moment in the excited state compared to that of ground state leading to preferential solvation of excited state over the ground state [30]. In NPCP, the fluorescence emission spectrum (Fig. 2) suffers a strong bathochromic shift as the solvent polarity increases. When the solvent is changed from cyclohexane to water, the emission maximum observably shift from 452–494 nm indicating that intensively photoinduced intramolecular charge transfer takes place within the molecule in the singlet excited state.

The fluorescence emission properties of NPCP-P follow a different trend. Fig. 3 presents the fluorescence spectra of NPCP-P in solvents of different polarity. It has been observed that increase of the polarity of aprotic solvents leads to a redshift of the emission wavelength, from 482 nm in cyclohexane to 506 nm in acetonitrile. Interestingly, the emission maximum of NPCP-P is strongly blue-shifted in highly polar protic solvent water. This result is opposite to a normal solvatochromic effect where the excited state is more stabilized in a more polar solvent giving rise to red-shifted emission bands. This result shows the hydrogen-bonding capability of the amide, which increases with the increasing proton donor ability of protic solvents. This is a well-known phenomenon occurring in aromatic amines, which is attributed to the hydrogen bonding interaction (more important in water, as

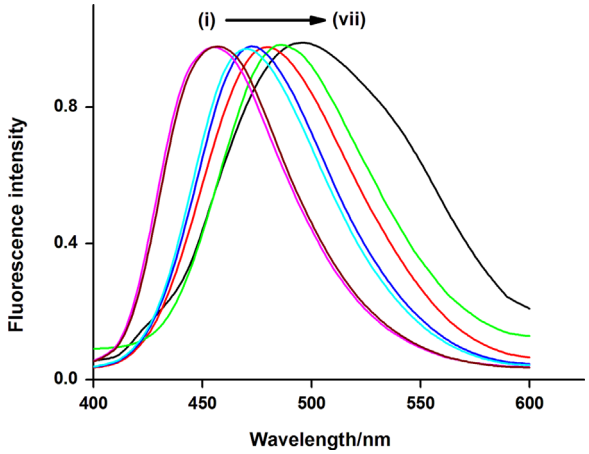

Fig. 2. Fluorescence spectra of NPCP in different homogeneous solvents; λ_{ex}=370 nm:. (i) n-heptane; (ii) n-cyclohexane; (iii) Dioxane; (iv)THF; (v) MeOH; (vi) Acetonitrile; (vii) water.

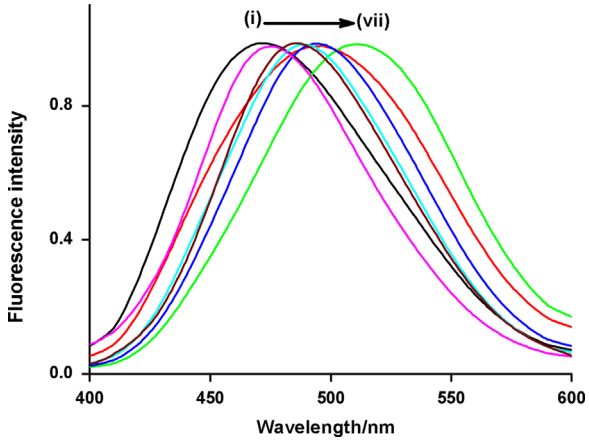

Fig. 3. Fluorescence spectra of NPCP-P in different homogeneous solvents; λ_{exc}=370 nm (i) water; (ii) n-Heptane; (iii) n-Cyclohexane; (iv) Dioxane; (v) THF; (vi) MeOH; (vii) Acetonitrile.

water has more hydrogen bonding sites than in alcohols) involving the lone pair of the terminal nitrogen atom. This is called the "blue-shift anomaly" observed in amino molecules dissolved in protic solvents [31]. The protic solvent acts as a hydrogen bond donor to the lone pair of the terminal amino group causing a reduced conjugation with the aromatic moiety.

Generally, the polarity of a solvent will influence the emission spectra of fluorophores by changes in quantum yields and Stokes shifts. The fluorescence quantum yields of NPCP and NPCP-P in different solvents are also investigated and are listed in Table 2. The data reveal a significant dependence of both compounds on the solvent properties, especially on E_T (30), (which measures both solvent polarizability and hydrogen bonding donating ability). The fluorescence quantum yield of both NPCP and NPCP-P increases with increasing solvent polarity from (0.47, 0.28) in a non-polar solvent cyclohexane to (0.55, 0.55) in a moderately polar solvent dioxane; with a further increase in solvent polarity the fluorescence quantum yield decreases with solvent polarity, (0.29, 0.17) in a strongly polar solvent-acetonitrile. Such a phenomenon of ϕ_f variation with solvent polarity indicates two mechanisms involved during the course of increasing polarity. One mechanism is the increase of ϕ_f with a suitable enhancement of ICT: the so-called "negative solvatokinetic effect" [32]. The proximity effect involving $n\pi$ electron configurations have been proposed to explain the "negative solvatokinetic effect" in NPCP and NPCP-P [33]. In other words, in non-polar solvents it will result in effective non-

radiative decay of the excited states. This effect is reduced with increase of solvent polarity. In strongly polar solvents, the "positive solvatokinetic effect" (reduction in ϕ_f by strong ICT) plays a predominant role so that the fluorescence quantum yield decreases with increase of solvent polarity due to the strong interaction between the strongly polarized molecule and solvents in the excited state [32]. Moreover, the much lower ϕ_f values in proton donor solvents can be attributed to the hydrogen bond interaction between the molecule and the surrounding solvent. This will induce fluorescence quenching due to the enhancement of intersystem crossing, strong internal conversion and vibrational deactivation. The long lifetimes of both compounds suggest that the emissions originate from intermolecular charge transfer state which is a stable and long-lived charge-separated state due to strong CT interactions inhibiting efficiently the back electron transfer [34].

Conclusively, the Stokes shift of both compounds in different solvents seems to be governed by three driving forces: solvent state polarity, hydrogen bonding and ICT. It may also be noted that the Stokes shift of both compounds observed in more polar acetonitrile is higher than that of protic water and methanol. This clearly indicates that the dipolar interaction predominate over the hydrogen bonding interaction and is due to ICT nature of the excited state [35]. Since Stokes shift ($\Delta\bar{\nu}$), the difference between transition energy corresponding to the absorption maxima E (A) and fluorescence maxima E (F), usually better correlated to the microscopic solvent polarity parameter E_T (30), the plot of the Stokes shift *versus* E_T (30) produces two distinct set of straight lines (Fig. 4) which suggest out of doubt that the types of interactions present in these two separate classes of solvents are different in nature (For NPCP-P cyclohexane is excluded from the list). In polar aprotic solvents only dipolar interaction is present whereas in polar protic solvents both dipolar and hydrogen bonding interactions are operating for the stabilization of the CT state.

We also observed the effect of specific solvent-fluorophore interactions by examining the emission spectra of NPCP and NPCP-P, (Fig. 5 and 6) in dioxane-water mixtures of different composition. After addition of water to dioxane solution of NPCP, the fluorescence intensity is found to be gradually increased accompanied by a red-shift (13 nm) of the emission maximum. This was attributed to greater stabilization of the highly dipolar ICT excited state by the more polar water molecules. This initial rapid increase in fluorescence intensity is due to increased hydrogen bonded interaction, as more and more water molecules replace the dioxane molecules in the microenvironment. It is also noted that upon further addition of water (here 0.8%), the fluorescence intensities of NPCP decreased dramatically due to modification of

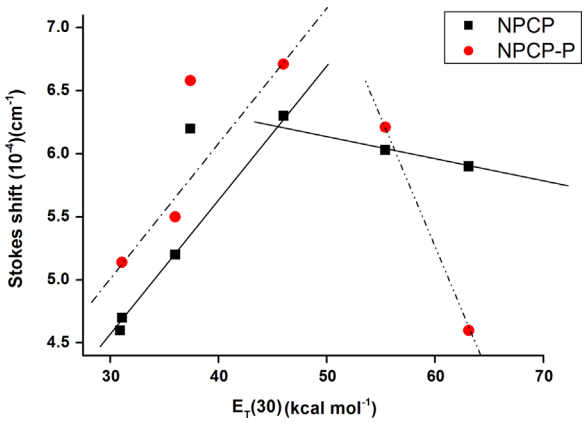

Fig. 4. Variation of the Stoke's shift with the polarity scale E_T (30).

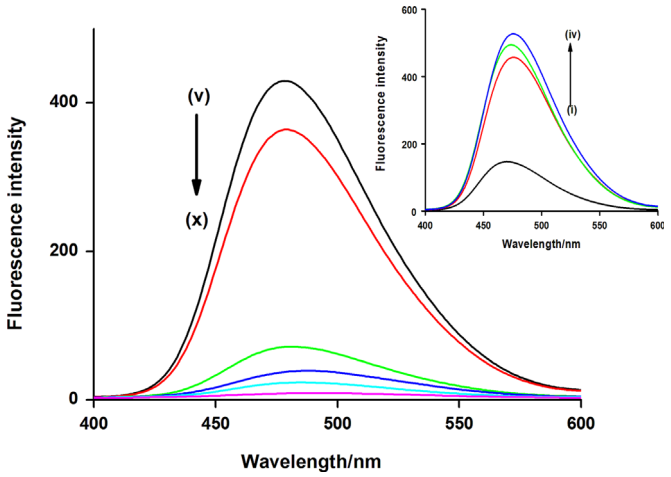

Fig. 5. Emission spectra of NPCP in 1, 4-dioxane as a function of water percentage composition. Inset represents the curves (i)–(iv) correspond to 0%, 0.1%, 0.2%, and 0.4% water (v/v), respectively; curves (v)–(x) correspond to 0.8%, 1%, 5%, 10%, 20%, and 40% respectively.

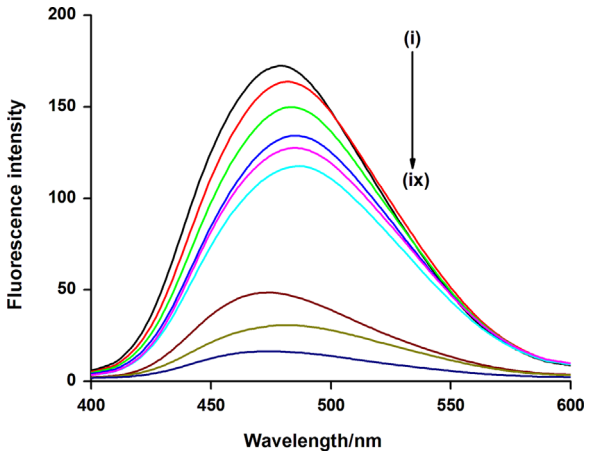

Fig. 6. Emission spectra of NPCP-P in 1, 4-dioxane as a function of water percentage composition. The curves (i)–(x) correspond to 0%, 0.1%, 0.2%, 0.4 0.8%, 1%, 5%, 10%, 20%, and 40% water (v/v) respectively.

water – NPCP hydrogen bonding interaction by the three-dimensional hydrogen bonded network present in liquid water. Owing to the strong self-association of water molecules, the microenvironment around fluorophore consists mainly of associated water clusters and these interact with the water molecules in the solvation shell, decreasing the hydrogen-bonding ability of bare water molecules. Such anomalous behaviour of water has also been reported in literature using other probes [36–38]. In case of NPCP-P, a progressive decrement of fluorescence intensity with slight redshift is observed on gradual water addition to the mixture. This should be the consequence of ground state clustering or of preferential hydrogen bonding of NPCP-P developing zwitterionic form of large dipole of the molecule and solvation of the excited solute dipole by polar water molecules.

Moreover, we used multiple linear regression methods to correlate the absorption (E_A) and emission (E_F) energies to the empirical solvent parameters; Taft's solvent parameter, π^* an index of the solvent dipolarity/polarizability, hydrogen bond donating ability of solvent, α, and hydrogen bond accepting ability of the solvent, β. For NPCP the regression analysis equations for the absorption and emission energies are as follows:

$$E_A = 76.1 - 2.18\alpha + 2.93\beta - 0.298\pi^* \quad \left(R^2 = 0.746\right) \tag{1}$$

$$E_F = 63.2 - 0.61\alpha + 0.118\beta - 4.126\pi^* \quad \left(R^2 = 0.923\right) \tag{2}$$

For NPCP-P the regression equations are as follows:

$$E_A = 78.4 - 2.05\alpha + 4.56\beta - 2.63\pi^* \quad \left(R^2 = 0.937\right) \tag{3}$$

$$E_F = 60.0 - 1.10\alpha + 4.60\beta - 6.45\pi^* \quad \left(R^2 = 0.855\right) \tag{4}$$

From the coefficients of these equations it can be inferred that these two compounds interact differently with solvents. It is apparent that the solvent dipolar interactions contribute significantly to the excited state properties of NPCP. This can be gleaned from a ratio of π^*/β of 35 for NPCP compared to a ratio of 1.4 for NPCP-P. Moreover, substantial hydrogen bonding predominates the excited state of NPCP-P compared to NPCP as can be seen from the coefficients of β. It is worth mentioning here that when water was included in the regression analysis of E_F for NPCP-P the correlation coefficient (R^2) obtained was 0.481 indicating that special interactions might have been occurring in water for the NPCP-P.

3.3. Effect of pH

The UV–visible absorption and emission characteristics of NPCP were measured in different pH ranging from 3 to 12. The NPCP shows significant dual absorption bands, (Fig. 7) the lower band is between 260 and 330 nm and the longer band is around 370 nm for pH ranging 6–12. From pH 5 onwards the absorption band experiences an appreciable red-shift on increasing the acidic nature of the buffer solution. On observing fluorescence spectra of NPCP (Fig. 8) at different pH, it is obvious that in strong acidic medium due to the protonation of the pyrazoline ring the fluorescence is almost quenched and slightly blue-shifted, while in basic medium the intensities are much higher. Also in acidic medium as a result of protonation, the new conjugated structure of NPCP was formed due to the charge redistribution [39]. Contrarily, under basic conditions the acid group of the proline moiety get deprotonated and causes an increase in fluorescence intensity due to stronger ICT effect.

The emission spectra of NPCP in various pH of aqueous buffer solution were also recorded. The acid dissociation constant of the dye in ground state ($pK_a = 10.36$) can be estimated by Henderson–Hasselbalch equation.

$$pH = pK_a + \log \frac{I - I_{min}}{I_{max} - I} \tag{5}$$

where I is the fluorescence intensity, I_{min} is the minimum fluorescence intensity in acidic form; I_{max} is the maximum fluorescence intensity in basic form and the dissociation constant in excited state were further calculated by the Förster equation [40].

$$pK_a^* = pK_a - hc\Delta\bar{\nu}, /2.3RT \tag{6}$$

where $\Delta\bar{\nu}$ is the wavenumber difference of transition energy between acidic and basic forms; R is the ideal gas constant; T is the temperature. The pK_a^* values calculated as 3.20 were smaller than the corresponding pK_a indicating their stronger acidity in the excited state.

3.4. Effect of surfactants

The emission spectrum of NPCP and NPCP-P were also measured in sodium dodecyl sulfate (SDS) anionic surfactants, cetyltrimethyl bromide (CTAB) cationic surfactants and Triton X-100 (TX-100) neutral surfactants. Figs. 9 and 10 presents the normalized emission spectra of NPCP and NPCP-P in surfactants and, for the sake of comparison, also in water. All surfactants used were maintained at concentrations above their critical micelle concentration (cmc)

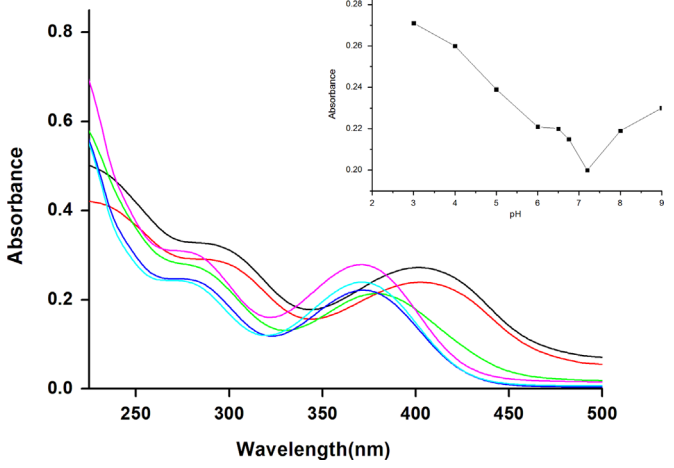

Fig. 7. The effect of pH on absorption spectra of NPCP. Curves from right to left are pH 3, 5, 6.75, 7.2, 9, and 12. Inset: effect of pH on the absorption intensity of NPCP.

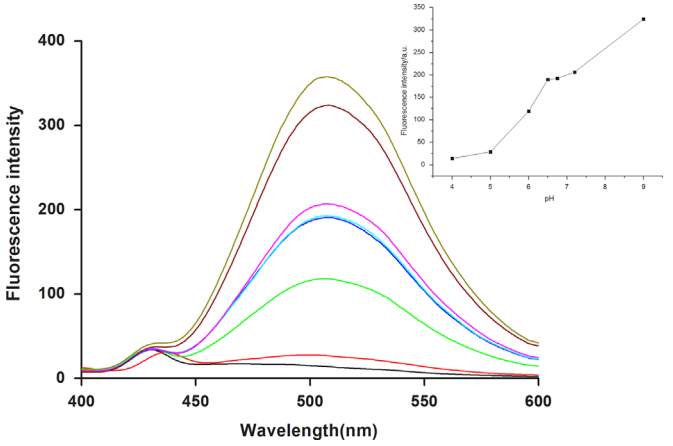

Fig. 8. The effect of pH on fluorescence spectra of NPCP. Curves from up to below are pH 12, 9, 7.2, 6.75, 6.5, 6, 5, and 4. Inset: plot of emission intensity at λ_{em} *versus* pH.

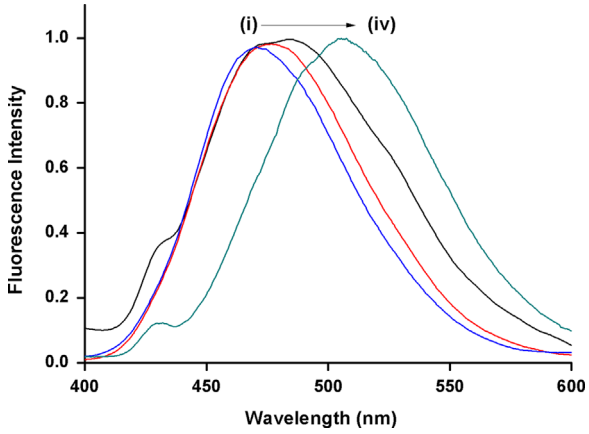

Fig. 9. Emission spectra of NPCP in (i) TX-100, (ii) CTAB, (iii) SDS, and (iv) water.

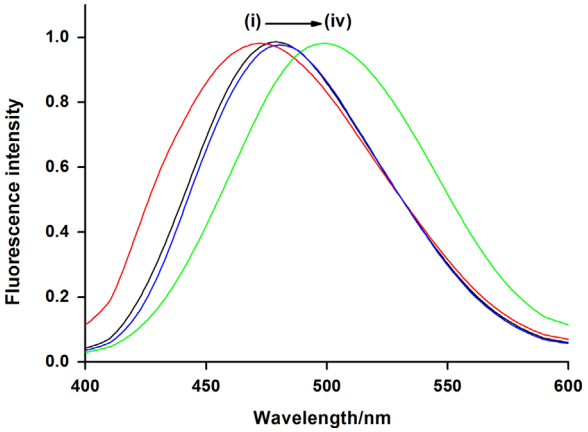

Fig. 10. Emission spectra of NPCP-P in (i) SDS, (ii) water, (iii) TX-100, and (iv) CTAB.

Table 3
Theoretically calculated geometrical parameters (B3LYP-6-31G(d, p)) of NPCP and NPCP-P in the ground and excited state.

Bond length Å/ Dihedral angle°	NPCP		NPCP-P	
	Ground state	Excited state	Ground state	Excited state
C6–C11	1.480	1.417	1.478	1.434
C11–C12	1.526	1.512	1.526	1.518
C12–C13	1.553	1.541	1.552	1.543
C13–N14	1.468	1.467	1.469	1.469
N14–N15	1.362	1.330	1.372	1.341
N15–C11	1.298	1.332	1.299	1.332
N14–C16	1.398	1.398	1.404	1.399
C13–C22	1.528	1.532	1.516	1.525
C5–C6–C11–C12	178.6	177.4	179.7	179.7
C18–C16–N14–N15	174.2	165.9	166.4	167.6
C12–C13–C22–C24	−70.5	75.3	92.2	92.2

The fluorescence band maximum of NPCP in water is strongly blue-shifted on adding SDS, CTAB and TX-100 (26, 28, and 36 nm respectively). It has been shown that NPCP possess a fluorescence ICT excited state; therefore, lowering the polarity of the medium destabilizes this state more than the ground state. As a consequence, the energy gap between the emitting and the ground state increases, thus, the emission maximum is shifted to the blue side. This shift is also accompanied by greater enhancement of emission intensity relative to that in water. As the probe enters the micelle from bulk water the hydrogen bond gets broken in less polar hydrophobic environment and thereby the radiationless transition become less active and enhancement of ICT emission in all micelles happens. This behaviour is also due to frictional forces and decreasing of solvent-free volume required for free rotations which are responsible for fluorescence quenching [41]. It has been observed that the intensity of NPCP in SDS is relatively lower than that of neutral micelle, TX-100. In the case of the anionic SDS micelle, the negatively charged head groups will repel the negative charge density on the carbonyl oxygen while the other part being sterically hindered cannot come close to the micelle. On the other hand, for TX-100 micelle H-bonding rather than electrostatic interaction is important and the unhindered oxygen can come close to the micelle leading to greater interaction.

In contrast, the fluorescence emission maximum for NPCP-P in CTAB is red-shifted compared to that of SDS and TX-100. This red-shifted fluorescence emission for NPCP-P in CTAB can be due to the involvement of polar, conformationally relaxed intramolecular charge transfer states, whose stability is expected to be influenced by changing micropolarity of the micelle domains. In addition to polarity, hydrogen bonding effect also plays a role at the binding site. So it is clear that NPCP-P in CTAB can be located in interfacial regions with 3-naphthyl-1-phenyl-2-pyrazoline fragment inside hydrophobic alkyl chains and with amide group towards polar environment favouring efficient hydrogen bonding. The peak position of NPCP-P in TX-100 is around 479 nm, which is very close to the emission peak of NPCP-P in water indicating that the interaction of the dye with the terminal –OH groups is important. The fluorescence quenching and blue shift in the fluorescence maximum of NPCP-P in SDS micelle suggested that the amide group is present in the stern layer and thus ion-dipole interaction may lead to fluorescence quenching.

3.5. *Theoretical calculations*

Using quantum chemical calculations both compounds, NPCP and NPCP-P, were optimized in the ground and excited states. In addition, TD-DFT calculations of the excited and ground states were performed. The optimized geometrical structures of title compounds are shown in Fig. S2. Selected geometrical parameters, such as bond length, and dihedral angles are compiled in Table 3. These parameters are consistent with those reported for other similar phenyl substituted pyrazoline compounds [18,42,43]. The bond length of the C–C single bond bridging the naphthalene and the pyrazoline groups is calculated to be 1.480 Å and 1.478 Å for PNCP and PNCP-P respectively. This bond is significantly shorter compared to a typical C–C single bond, 1.54 Å. These bonds were shortened further in the excited state by 0.063 Å and 0.044 Å for NPCP and NPCP-P respectively. This reflects the efficient charge delocalization over the pyrazoline π-system allowing the electronic interaction between the naphthalene group and the aryl substituents albeit they are electronically separated. The electron lone pair on the pyrazoline N14 atom can be easily delocalized towards the naphthalene and the aryl substituents. The delocalization of the electron density of the pyrazoline ring to the substituted phenyl group at N14 is further supported by the shortened N14-C16 bond.

From the dihedral angles shown in Table 3 it is clear that the phenyl and the naphthalene substituents adopt a nearly coplanar orientation with the pyrazoline ring. Such an orientation is expected to allow for efficient electronic interaction between these groups. On the other hand, the dipole moments of each compound were calculated (Table 3), where the structures in the excited state exhibited higher diploe moments in comparison to the ground state. These observations are in line with the experimental results, as these compounds demonstrated positive solvatochromic effect when the polarity of the solvent was increased.

Figs. S3 and S4 show the orbital shapes of the highest occupied molecular orbitals (HOMOs) and lower molecular orbitals (LUMOs) of NPCP and NPCP-P, respectively. It is apparent from these figures that the HOMO plots and LUMO plots of the two compounds are similar. In all cases the HOMO electron density is mainly localized on phenyl group, pyrazoline (N14–N15–C11) and C1–C6–C5 of the naphthalene group. On the other hand, LUMO electron density is localized on the naphthalene ring. This is indicative of the tendency for intramolecular charge transfer which contains the pyrazoline lone pair. It is apparent from these plots the lowest absorption and emission electronic transitions of the lowest singlet states involves a $\pi\pi^*$ type.

The calculated results for the first singlet excitation energies and oscillator strengths are summarized in Table 4. The calculated absorption wavelengths are in reasonable agreement with the experimental results; however, a slight red-shift for the calculated lower energy wavelengths was obtained. The lower energy optical transition corresponds to HOMO→LUMO (100%) component for NPCP-P. For NPCP this transition originates mainly from

Table 4
HOMO–LUMO energies, HOMO–LUMO energy gap (E_g), absorption and emission wavelengths, oscillator strengths and dipole moments calculated at TDB3LYP level for NPCP and NPCP-P.

Parameter	NPCP		NPCP-P	
	Ground state	Excited state	Ground state	Excited state
E_{HOMO}(eV)	−4.903	−4.708	−4.890	−4.710
E_{LUMO}(eV)	−1.586	−1.742	−1.542	−1.674
E_g(eV)	3.312	2.966	3.348	3.036
λ_1(nm)/f	409.0/0.5213	443.4/0.6196	406.8/0.5282	451.7/0.5810
λ_2(nm)/f	293.8/0.0861	–	290.9/0.1006	–
μ (Debye)	3.094	3.304	3.846	5.689

HOMO→LUMO (90%) and a minor contribution from HOMO→L+1 (10%). The calculated emission wavelengths for both compounds are blue-shifted compared to the experimentally obtained results. In both cases the emission transitions are mainly HOMO→LUMO transitions. It worth noting here that in this work the effect of the solvent was not taken into consideration.

4. Conclusions

A new pyrazoline based probe 3-naphthyl-1-phenyl-5-(4-carboxyphenyl)-2-pyrazoline (NPCP), and its proline derivative (NPCP-P) has been synthesized and characterized. Several interesting aspects of the photophysical properties of these compounds have been described and specific solvent–fluorophore interactions were also identified by examining the emission spectra in a variety of solvents. Extremely high solvatochromism of the normal emission band of the NPCP makes it one of the most effective solvatochromic dyes in the pyrazoline family. Moreover, we found that the incorporation of amino group (NPCP-P) leads to considerable changes in the spectral response and fluorescence efficiency of the systems in comparison with the unsubstituted analog (NPCP). The interaction of NPCP and NPCP-P in different micellar solution brings out the difference in the behavioral pattern of compounds in various medium. The results obtained from the quantum chemical calculations supported the experimentally observed properties of the title compounds. From these calculations it was inferred that the charge transfer character of these compounds originate from the facile interaction of the distant phenyl and naphthyl groups across the pyrazoline ring. Keeping in mind the wide spread applications of pyrazoline derivatives in biomedical fields, the photophysical study of this newly synthesized compounds will help in assessing their potential application in different environments.

Acknowledgment

BV thanks Sultan Qaboos University for PhD scholarship and financial support.

Appendix A. Supporting information

Supplementary data associated with this article can be found in the online version at http://dx.doi.org/10.1016/j.jlumin.2014.10.045.

References

[1] S.-Q. Wang, Y. Gao, H.-Y. Wang, X.-X. Zheng, S.-L. Shen, Y.-R. Zhang, B.-X. Zhao, Spectrochim. Acta Part A: Mol. Biomol. Spectrosc. 106 (2013) 110.
[2] S.Q. Wang, Q.H. Wu, H.Y. Wang, X.X. Zheng, S.L. Shen, Y.R. Zhang, J.Y. Miao, B.X. Zhao, Analyst 138 (2013) 7169.
[3] J. Mysliwiec, A. Szukalski, L. Sznitko, A. Miniewicz, K. Haupa, K. Zygadlo, K. Matczyszyn, J. Olesiak-Banska, M. Samoc, Dyes Pigments 102 (2013) 63.
[4] D. Secci, S. Carradori, A. Bolasco, B. Bizzarri, M. D'Ascenzio, E. Maccioni, Curr. Top. Med. Chem. 12 (2012) 2240.
[5] J. Mysliwiec, A. Szukalski, L. Sznitko, A. Miniewicz, K. Haupa, K. Zygadlo, K. Matczyszyn, J. Olesiak-Banska, M. Samoc, Dyes Pigments 102 (2014) 63.
[6] P. Singh, J.S. Negi, K. Singh, G.J. Pant, M.S.M. Rawat, G.C. Joshi, Synth. Metals 162 (2012) 1977.
[7] J. Li, D. Li, Y. Han, S. Shuang, C. Dong, Spectrochim. Acta Part A: Mol. Biomol. Spectrosc. 73 (2009) 221.
[8] J. Barberá, K. Clays, R. Giménez, S. Houbrechts, A. Persoons, J.L. Serrano, J. Mater. Chem. 8 (1998) 1725.
[9] S.P. Sakthinathan, G. Vanangamudi, G. Thirunarayanan, Spectrochim. Acta Part A: Mol. Biomol. Spectrosc. 95 (2012) 693.
[10] A. Abbas, H. Nazir, M.M. Naseer, M. Bolte, S. Hussain, N. Hafeez, A. Hasan, pectrochim. Acta Part A: Mol. Biomol. Spectrosc. 120 (2014) 176.
[11] S.S. Mati, S. Sarkar, S. Rakshit, A. Sarkar, S.C. Bhattacharya, RSC Adv. 3 (2013) 8071.
[12] S.Y. Jadhav, S.P. Shirame, S.D. Kulkarni, S.B. Patil, S.K. Pasale, R.B. Bhosale, Bioorg. Med. Chem. Lett. 23 (2013) 2575.
[13] S.N.A. Bukhari, I. Jantan, L.K. Wai, N.H. Lajis, F. Abbas, M. Jasamai, Med. Chem. 9 (2013) 1091.
[14] F.M. Awadallah, G.A. Piazza, B.D. Gary, A.B. Keeton, J.C. Canzoneri, Eur. J. Med. Chem. 70 (2013) 273.
[15] R. Aggarwal, A. Bansal, I. Rozas, B. Kelly, P. Kaushik, D. Kaushik, Eur. J. Med. Chem. 70 (2013) 350.
[16] P.-C. Lv, D.-D. Li, Q.-S. Li, X. Lu, Z.-P. Xiao, H.-L. Zhu, Bioorg. Med. Chem. Lett. 21 (2011) 5374.
[17] Z.A. Kaplancikli, G. Turan-Zitouni, A. Özdemir, Ö.D. Can, P. Chevallet, Eur. J. Med. Chem. 44 (2009) 2606.
[18] C.J. Fahrni, L. Yang, D.G. VanDerveer, J. Am. Chem. Soc. 125 (2003) 3799.
[19] Y. Zhenglin, W. Shikang, J. Lumin. 54 (1993) 303.
[20] W. Seebacher, G. Michl, F. Belaj, R. Brun, R. Saf, R. Weis, Tetrahedron 59 (2003) 2811.
[21] A.D. Becke, Phys. Rev. A 38 (1988) 3098.
[22] C. Lee, W. Yang, R.G. Parr, Phys. Rev. B: Condens. Matter 37 (1988) 785.
[23] J.B. Forseman, M. Head-Gordon, J.A. Pople, M.J. Frisch, J. Phys. Chem. 96 (1992) 135.
[24] Granovsky A.A., Firefly version 8.0 ⟨http://classic.chem.msu.su/gran/firefly/index.html⟩.
[25] M.W. Schmidt, K.K. Baldridge, J.A. Boatz, S.T. Elbert, M.S. Gordon, J.H. Jensen, S. Koseki, N. Matsunaga, K.A. Nguyen, S. Su, T.L. Windus, M. Dupuis, J.A. Montgomery, J. Comput. Chem. 14 (1993) 1347.
[26] N.M. O'boyle, A.L. Tenderholt, K.M. Langner, J. Comput. Chem. 29 (2008) 839.
[27] A.-R. Allouche, J. Comput. Chem. 32 (2011) 174.
[28] A. Sarkar, T.K. Mandal, D.K. Rana, S. Dhar, S. Chall, S.C. Bhattacharya, J. Lumin. 130 (2010) 2271.
[29] Z. Li, Q. Yang, R. Chang, G. Ma, M. Chen, W. Zhang, Dyes Pigments 88 (2011) 307.
[30] Z.-L. Gong, L.-W. Zheng, B.-X. Zhao, D.-Z. Yang, H.-S. Lv, W.-Y. Liu, S. Lian, J. Photochem. Photobiol. A: Chem. 209 (2010) 49.
[31] P. Pal, H. Zeng, G. Durocher, D. Girard, R. Giasson, L. Blanchard, L. Gaboury, L. Villeneuve, J. Photochem. Photobiol. A: Chem. 98 (1996) 65.
[32] M. Danko, A. Andics, C. Kosa, P. Hrdlovic, D. Vegh, Dyes Pigments 92 (2012) 1257.
[33] H.D. Becker, K. Sandros, B.W. Skelton, A.H. White, J. Phys. Chem. 85 (1981) 2927.
[34] H.u.X. Zhang H-h, W. Dou, W.-s. Liu, J. Fluor. Chem. 131 (2010) 883.
[35] M. Gaber, Y.S. El-Sayed, H. Diab, Opt. Laser Technol. 43 (2011) 592.
[36] A.K. Mitra, S. Ghosh, S. Chakraborty, S. Basu, C. Saha, J. Lumin. 143 (2013) 693.
[37] S. Chatterjee, P. Banerjee, S. Pramanik, A. Mukherjee, K.K. Mahalanabis, S.C. Bhattacharya, Chem. Phys. Lett. 440 (2007) 313.
[38] T.A. Fayed, Colloids Surf. A: Physicochem. Eng. Aspects 236 (2004) 171.
[39] J.F. Li, B. Guan, D.X. Li, C. Dong, Spectrochim. Acta Part A: Mol. Biomol. Spectrosc. 68 (2007) 404.
[40] L.M. Tolbert, K.M. Solntsev, Acc. Chem. Res. 35 (2002) 19.
[41] M.R. Popović, G.V. Popović, D.D. Agbaba, J. Chem. Eng. Data 58 (2013) 2567.
[42] S. Easwaramoorthi, B. Umamahesh, P. Cheranmadevi, R.S. Rathore, K.I. Sathiyanarayanan, RSC Adv. 3 (2013) 1243.
[43] S.S. Mati, S. Sarkar, P. Sarkar, S.C. Bhattacharya, J. Phys. Chem. A 116 (2012) 10371.